

Electronic Supplementary Information:

Electrochromic Second-Order NLO Chromophores based on M^{II} ($M = Ni, Pd, Pt$) Complexes with Diselenolato-Dithione (Donor-Acceptor) Ligands

Davide Espa,^a Luca Pilia,^{a,b} Luciano Marchiò,^c Maddalena Pizzotti,^d Neil Robertson,^b Francesca Tessore,^d M. Laura Mercuri,^a Angela Serpe^a and Paola Deplano.^{a*}

^aDipartimento di Scienze Chimiche e Geologiche, Università di Cagliari, Unità di Ricerca dell'INSTM, S.S. 554-Bivio per Sestu, I09042 Monserrato-Cagliari, Italy

^bEaStChem and School of Chemistry, University of Edinburgh, King's Buildings, West Mains Road, Edinburgh EH9 3JJ, UK;

^cDipartimento di Chimica Generale ed Inorganica, Chimica Analitica, Chimica Fisica, Università di Parma, Parco Area delle Scienze 17A, I43100 Parma, Italy

^dDipartimento di Chimica, Università di Milano, Unità di Ricerca dell'INSTM, via Golgi 19, 20133 Milano, Italy

e-mail: deplano@unica.it

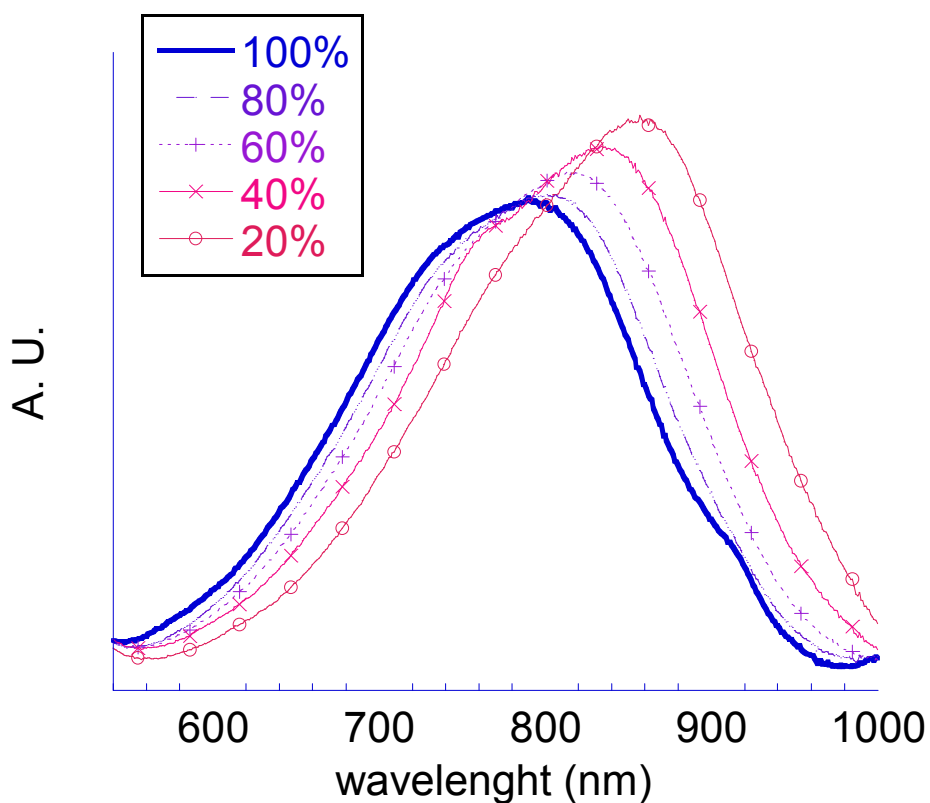


Figure S1. Solvatochromic behaviour of $[\text{Pt}(\text{Bz}_2\text{pipdt})(\text{dsit})]$ **3** in DMF/ CS_2 mixtures ranging from DMF 100% to 20%. The energy of the solvatochromic peak of **3** versus the solvent polarity parameter for solutions from DMF 100% to 20% follows a straight line with slope 1.2.

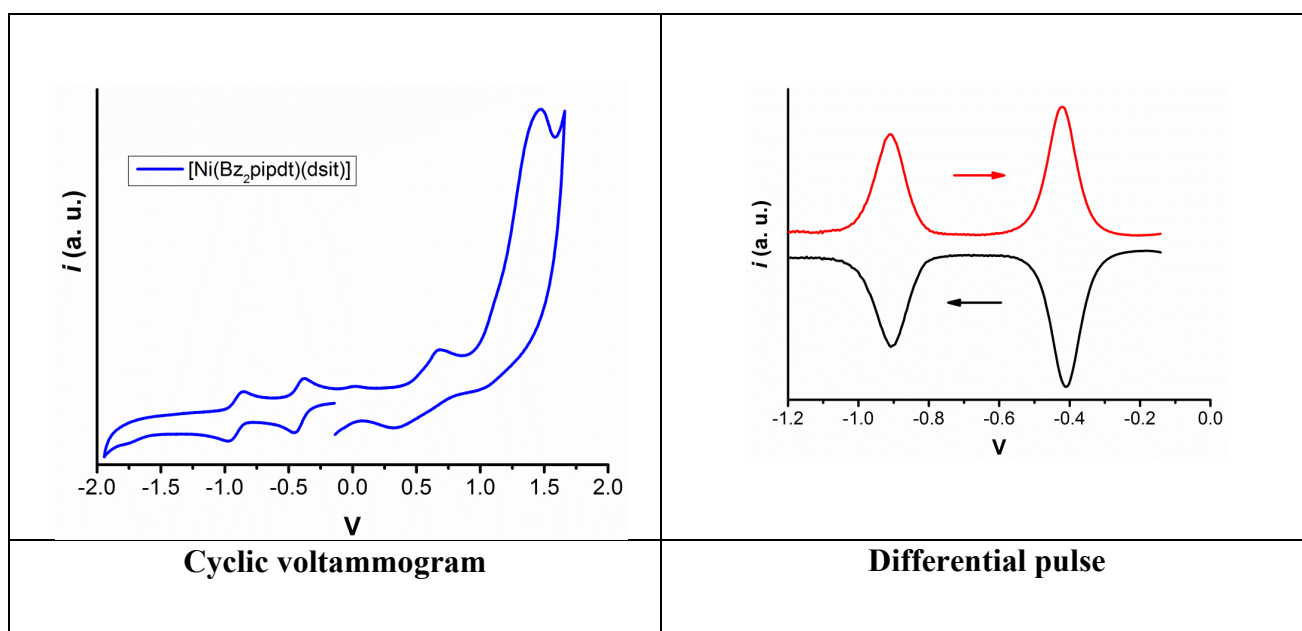


Figure S2. Electrochemical measurements on DMF solution of $[\text{Ni}(\text{Bz}_2\text{pipdt})(\text{dsit})]$ **1** containing 0.1 M TBABF_4

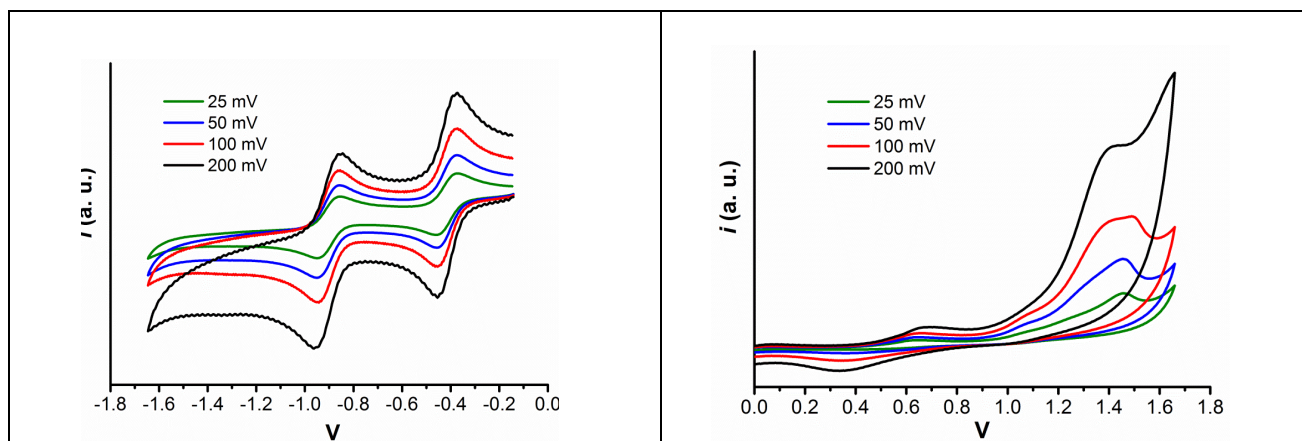


Figure S3. Cyclic voltammogram in a DMF solution of **1** containing 0.1 M TBABF₄ at 298 K at different scan rates.

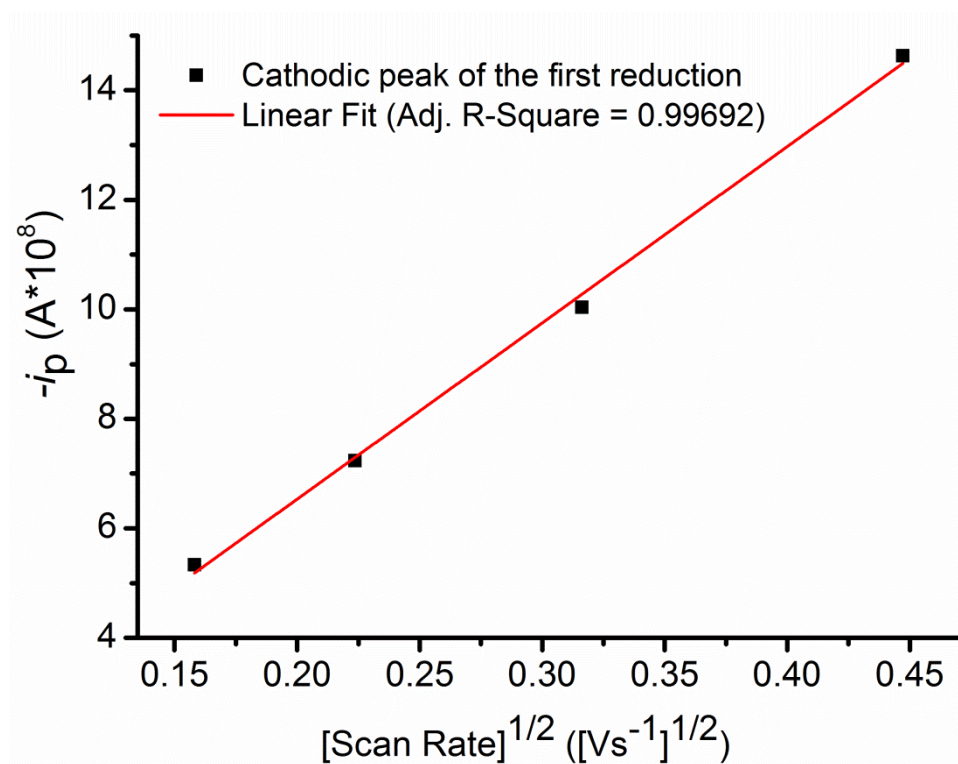
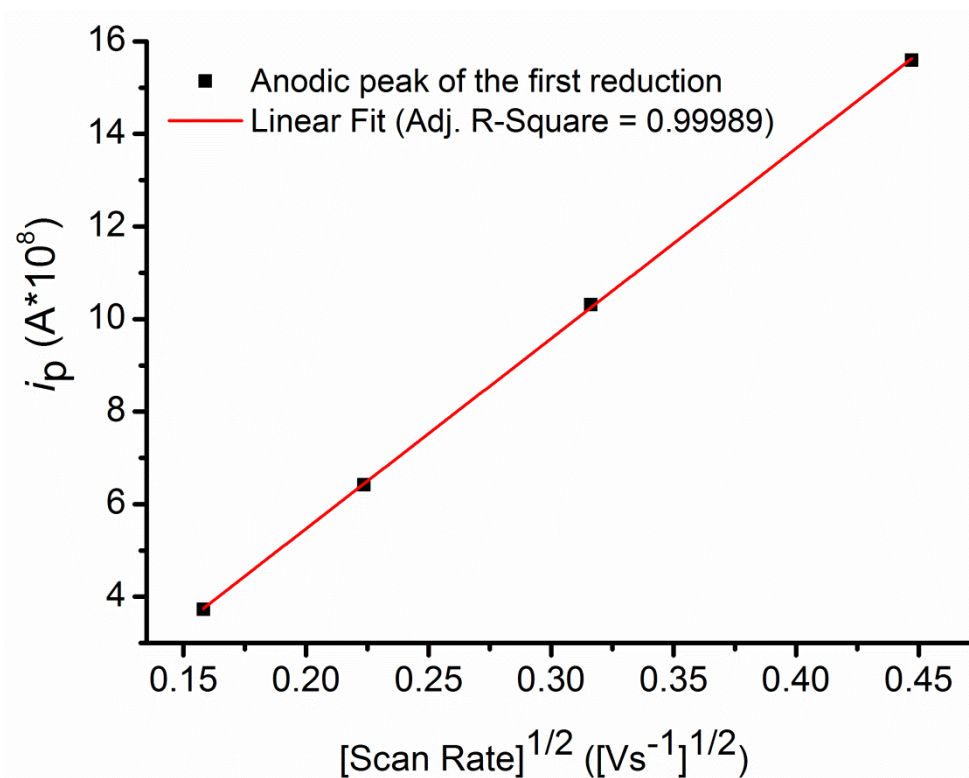


Figure S4. Linear dependence of the anodic peak (above) and cathodic peak (below) currents of the first reduction from the square root of the voltage scan rate in the case of complex **1**, [Ni(Bz₂pipdt)(dsit)].

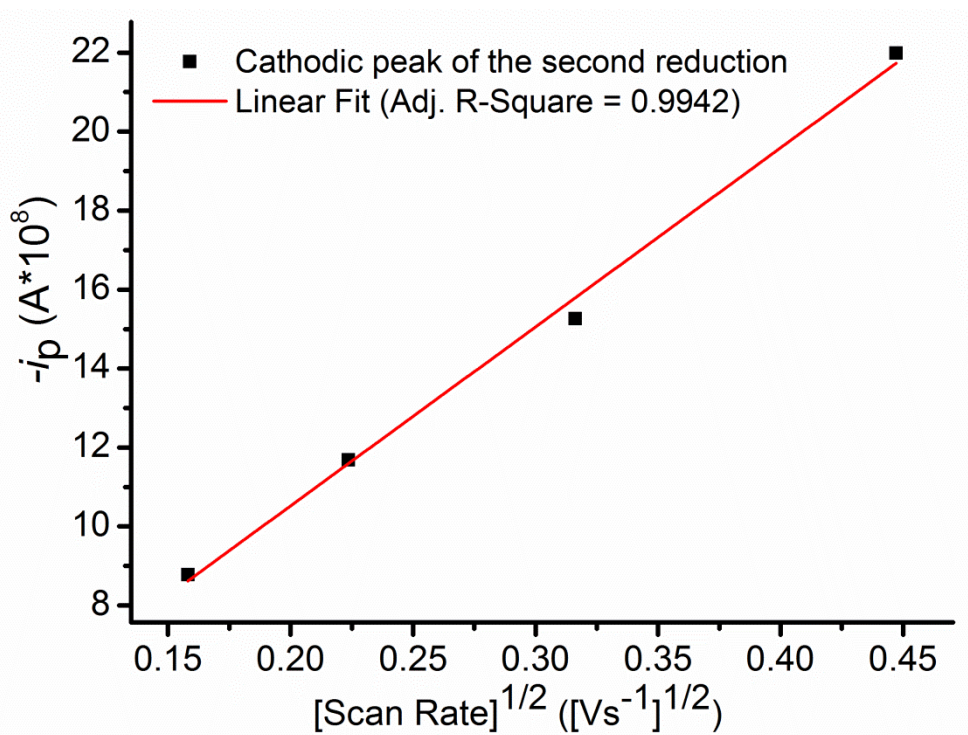
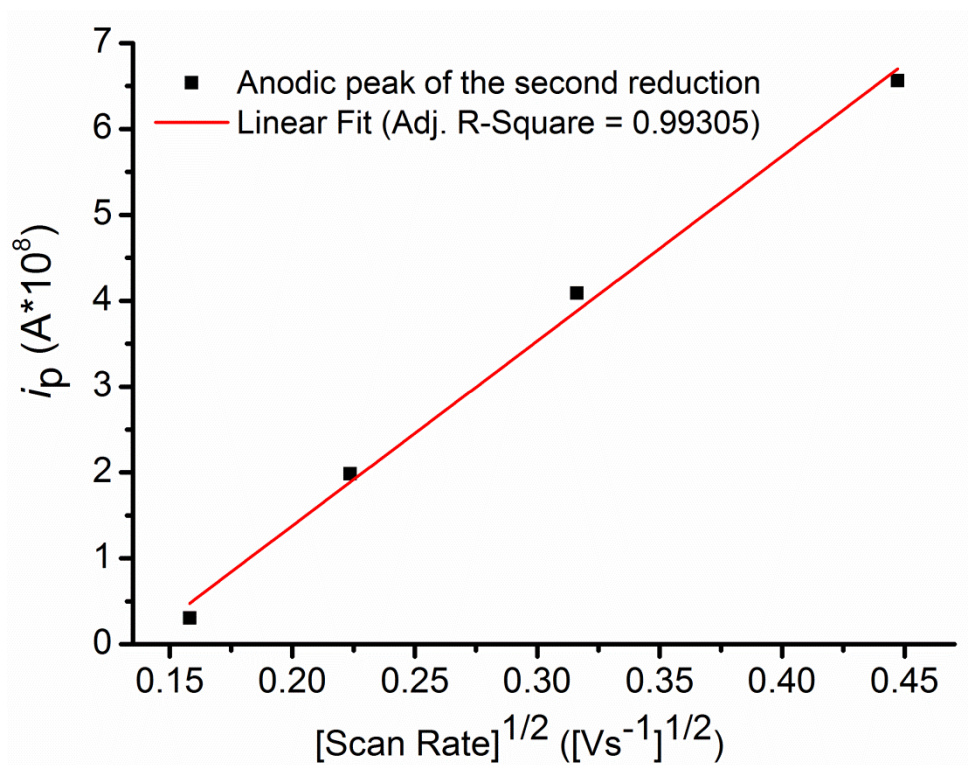


Figure S5. Linear dependence of the anodic peak (above) and cathodic peak (below) currents of the second reduction from the square root of the voltage scan rate in the case of complex **1**, $[Ni(Bz_2pipdt)(dsit)]$.

Table S1 Selected Experimental and calculated bond distances (Å) and angles (deg) for [Ni(Bz₂pipdt)(dsit)] (**1**), [Pd(Bz₂pipdt)(dsit)] (**2**), and [Pt(Bz₂pipdt)(dsit)] (**3**).

	[Ni(Bz ₂ pipdt)(dsit)] (1)		[Pd(Bz ₂ pipdt)(dsit)] (2)		[Pt(Bz ₂ pipdt)(dsit)] (3)	
	Exp.	Calc.	Exp.	Calc.	Exp.	Calc.
M-Se (dsit)	2.2884(8)	2.309	-	2.427	2.3939(9)	2.436
	2.2755(8)	2.309		2.427	2.4034(9)	2.436
M-S (R₂pipdt)	2.151(1)	2.197	-	2.335	2.264(2)	2.335
	2.162(1)	2.197		2.335	2.276(2)	2.335
Se-C (dsit)	1.876(5)	1.883	-	1.890	1.896(7)	1.890
	1.880(5)	1.883		1.890	1.883(7)	1.890
S-C (R₂pipdt)	1.691(5)	1.711	-	1.713	1.676(7)	1.715
	1.673(5)	1.711		1.713	1.690(8)	1.715
C-C (dsit)	1.355(6)	1.367	-	1.365	1.347(9)	1.361
	1.490(6)	1.460		1.467	1.491(9)	1.454
C-N (R₂pipdt)	1.323(5)	1.362	-	1.363	1.318(9)	1.365
	1.328(5)	1.362		1.363	1.353(9)	1.365
Se-M-Se (dsit)	94.44(3)	94.10	-	91.04	92.21(3)	90.79
S-M-S (R₂pipdt)	91.10(5)	90.66	-	86.85	88.22(7)	86.46
M-Se-C (dsit)	100.4(1)	100.62	-	100.75	99.8(2)	100.70
	101.0(2)	100.62		100.75	100.0(2)	100.70
M-S-C (R₂pipdt)	106.4(2)	105.54	-	105.93	106.2(3)	106.18
	106.0(2)	105.54		105.93	106.0(2)	106.18
Se-C-C (dsit)	122.7(4)	122.33	-	123.73	123.4(6)	123.91
	122.8(3)	122.33		123.73	124.5(6)	123.91
S-C-C (R₂pipdt)	114.6(4)	119.03	-	120.48	119.0(6)	120.54
	117.2(4)	119.03		120.48	120.3(6)	120.54

Table S2. Spatial plots of relevant MOs (isovalue= 0.04) of [Ni(Bz₂pipdt)(dsit)] in DMF (B3LYP/6-311G(d,p)-SDD).

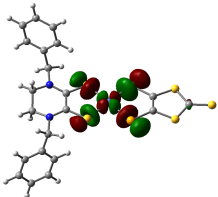
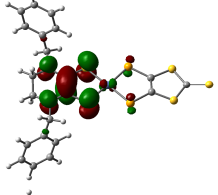
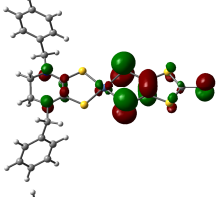
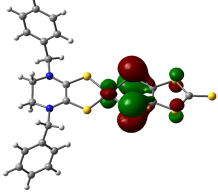
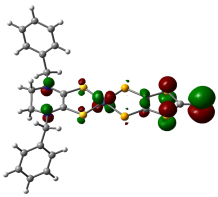
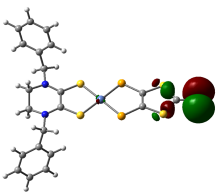
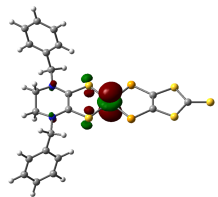
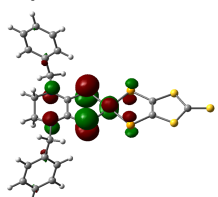
		E (eV)
LUMO+1		-2.51
LUMO		-3.68
HOMO		-5.34
HOMO-1		-6.26
HOMO-2		-6.57
HOMO-3		-6.63
HOMO-4		-6.80
HOMO-5		-6.86

Table S3. Spatial plots of relevant MOs (isovalue= 0.04) of [Pd(Bz₂pipdt)(dsit)] in DMF (B3LYP/6-311G(d,p)-SDD).

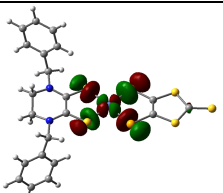
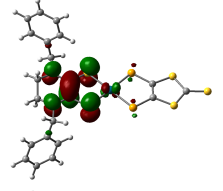
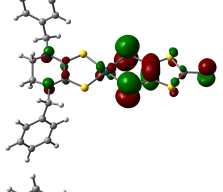
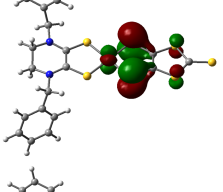
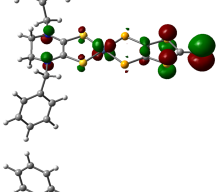
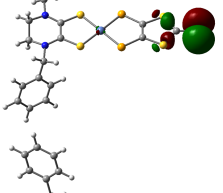
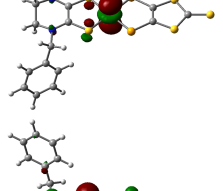
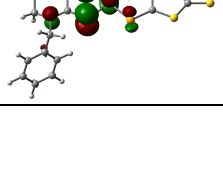
		E (eV)
LUMO+1		-2.61
LUMO		-3.75
HOMO		-5.30
HOMO-1		-6.22
HOMO-2		-6.62
HOMO-3		-6.64
HOMO-4		-6.91
HOMO-5		-6.95

Table S4. Spatial plots of relevant MOs (isovalue= 0.04) of [Pt(Bz₂pipdt)(dsit)] in DMF (B3LYP/6-311G(d,p)-SDD).

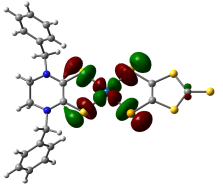
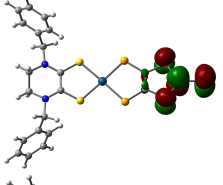
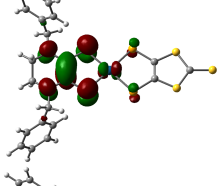
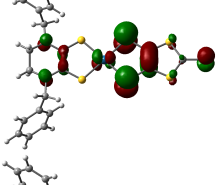
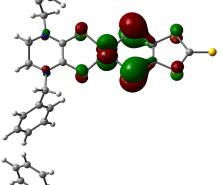
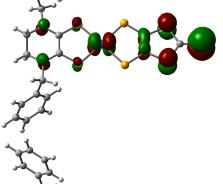
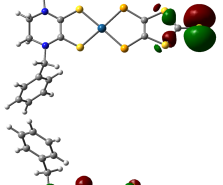
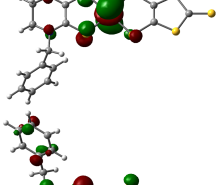
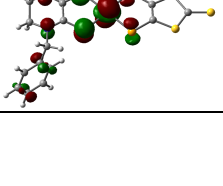
		E (eV)
LUMO+2		-2.09
LUMO+1		-2.14
LUMO		-3.74
HOMO		-5.32
HOMO-1		-6.10
HOMO-2		-6.53
HOMO-3		-6.62
HOMO-4		-6.92
HOMO-5		-6.96

Table S5 TD-DFT calculated energies and compositions of the lowest lying singlet electronic transitions of $[M(\text{Bz}_2\text{pipdt})(\text{dsit})]$, ($M = \text{Ni}, \text{Pd}, \text{Pt}$) complexes in DMF, (B3LYP/6-311G(d,p)-SDD). The principal singlet transition responsible for the main absorption band in the visible region is shown in bold.

Compound	State	Composition ^a	ΔE (eV/nm) ^b	f^c	Character
[Ni(Bz₂pipdt)(dsit)]	1	HOMO → LUMO 74%	1.36 / 914	0.3075	dsit/Ni/Bz₂pipdt → dsit/Ni/Bz₂pipdt (MMLL'CT)
	2	HOMO → LUMO+1 60% HOMO-2 → LUMO+1 15%	1.66 / 745	0.0219	
	3	HOMO-1 → LUMO 43% HOMO-4 → LUMO+1 22% HOMO-5 → LUMO+1 9% HOMO-1 → LUMO+1 8%	1.68 / 737	0.0015	
	4	HOMO-1 → LUMO+1 35% HOMO-4 → LUMO+1 25% HOMO-4 → LUMO 14% HOMO-13 → LUMO+1 7%	1.77 / 699	0.0001	
	5	HOMO-1 → LUMO 14% HOMO-4 → LUMO 17% HOMO-1 → LUMO+1, 15% HOMO-5 → LUMO+1, 7%	1.97 / 630	0.0021	
[Pd(Bz₂pipdt)(dsit)]	1	HOMO → LUMO 78%	1.25 / 989	0.2376	dsit/Pd/Bz₂pipdt → dsit/Pd/Bz₂pipdt (MMLL'CT)
	2	HOMO → LUMO+1 93%	1.80 / 688	0.0125	
	3	HOMO-1 → LUMO 91% HOMO-4 → LUMO 89%	1.86 / 668	0.0037	
	4	HOMO-5 → LUMO 8% HOMO-2 → LUMO 80%	2.26 / 547	0.0002	
	5	HOMO-3 → LUMO 7%	2.47 / 502	0.0841	
[Pt(Bz₂pipdt)(dsit)]	1	HOMO → LUMO 75%	1.35 / 918	0.3318	dsit/Pt/Bz₂pipdt → dsit/Pt/Bz₂pipdt (MMLL'CT)
	2	HOMO-1 → LUMO 90% HOMO-4 → LUMO 88%	1.71 / 723	0.0043	
	3	HOMO-5 → LUMO 10% HOMO → LUMO+2 86%	2.23 / 557	0.0004	
	4	HOMO-2 → LUMO 9% HOMO-2 → LUMO 81%	2.35 / 527	0.0000	
	5	HOMO → LUMO+2 8%	2.42 / 512	0.0771	

^a Compositions of electronic transitions are expressed in terms of contributing excitations between groundstate Kohn–Sham molecular orbitals.

^b Transition energy from the ground state in eV. ^c Oscillator strength.

Table S6. Comparison of HOMO-LUMO energy in eV and energy gap between [Pt(Bz₂pipdt)(dmit)]^{7b} and [Pt(Bz₂pipdt)(dsit)] in DMF and in the gas-phase (in parenthesis).

dsit	HOMO	-5.32 (-4.99)
	LUMO	-3.74 (-3.69)
	Gap	1.58 (1.30)
dmit	HOMO	-5.26 (-4.96)
	LUMO	-3.74 (-3.70)
	Gap	1.52 (1.26)

Table S7. Calculated ground state dipole moments (μ_g) and $\Delta\mu_{ge}$ of [M(Bz₂pipdt)(dsit)], (M = Ni, Pd, Pt) complexes. CPCM (DMF) B3LYP/6-311G(d,p)-SDD. The $\Delta\mu_{ge}$ (in Debye) was calculated with the finite field approach.

Compound	Ground state	ge (FF)
[Ni(Bz₂pipdt)(dsit)]	18.9550 (void)	-8.34 (DMF)
	32.5138 (DMF)	
[Pd(Bz₂pipdt)(dsit)]	19.6285 (void)	-10.31 (DMF)
	33.6150 (DMF)	
[Pt(Bz₂pipdt)(dsit)]	18.8448 (void)	-8.66 (DMF)
	31.8462 (DMF)	